cells

MDPI

Article

Stromal cell signature associated with response to neoadjuvant chemotherapy in locally advanced breast cancer

Maria Lucia Hirata Katayama[1]*, René Aloísio da Costa Vieira[2]*, Victor Piana Andrade[3], Rosimeire Aparecida Roela[1], Luiz Guilherme Cernaglia Aureliano Lima[3], Ligia Maria Kerr[4], Adriano Polpo de Campos[5], Carlos Alberto de Bragança Pereira [6], Pedro Adolpho de Menezes Pacheco Serio[1], Giselly Encinas[1], Simone Maistro[1], Maria Mitzi Brentani[1], Maria Aparecida Azevedo Koike Folgueira [1].

[1] Departamento de Radiologia e Oncologia, Centro de Investigação Translacional em Oncologia, Instituto do Câncer do Estado de São Paulo, Hospital das Clinicas HCFMUSP, Faculdade de Medicina, Universidade de SaoPaulo, Sao Paulo, SP, Brazil
[2] Hospital de Câncer de Barretos, Barretos, SP, Brazil
[3] A.C. Camargo Cancer Center, São Paulo, SP, Brazil
[4] Departamento de Patologia. Hospital de Câncer de Barretos, SP, Brazil
[5] Departamento de Estatística, Centro de Ciências Exatas e de Tecnologia, Universidade Federal de São Carlos, São Carlos, SP, Brazil
[6.] Departamento de Estatística, Instituto de Matemática e Estatística, Universidade de São Paulo, SP, Brazil

* These authors participated equally in this work
Corresponding Author
Email: maria.folgueira@fm.usp.br (MAAKF)

ABSTRACT

There is evidence that the stromal compartment may influence breast cancer responsiveness to chemotherapy. Our aim was to detect a stromal cell signature (using a direct approach of microdissected stromal cells) associated with response to neoadjuvant chemotherapy in locally advanced breast cancer. Forty four patients with locally advanced breast cancer (29 ER positive and 15 ER negative) were included. Neoadjuvant chemotherapy consisted of doxorubicin/cyclophosphamide, followed by paclitaxel. Response was defined as downstaging to maximum ypT1a-b/ypN0. Stromal cells were microdissected from fresh frozen tumor samples and gene expression profile was determined using Agilent SurePrint G3 Human Gene Expression Microarrays. Expression levels were compared using MeV (MultiExperiment Viewer) software, applying SAM (Significance analysis of microarrays). To classify samples according to tumor response, the order of median based on confidence statements (MedOr), was used and to identify gene sets correlated with the phenotype downstaging, gene set enrichment analysis (GSEA). Nine patients presented disease downstaging. Eleven sequences (FDR 17) were differentially expressed, all of which (except *H2AFJ*) more expressed in responsive tumors, including *PTCHD1* and genes involved in abnormal cytotoxic T cell physiology: *TOX*, *LY75*, *SH2D1A*. Four pairs of markers could correctly classify all tumor samples according to response: *PTCHD1/PDXDC2P; LOC100506731/NEURL4*; *SH2D1A/ENST00000478672; TOX/H2AFJ*. Gene sets correlated with

tumor downstaging (FDR < 0.01) were mainly involved in immune response or lymphocyte activation. In locally advanced breast cancer, stromal cells may present specific features of immune response that may be associated with chemotherapy response.

Key Words: Breast cancer, stromal cells, Gene expression, Chemotherapy neoadjuvant

1. INTRODUCTION

Neoadjuvant chemotherapy has a central role in the management of locally advanced breast cancer and a number of different response predictive signatures have been identified, however, to the present moment, none of them is used in the clinical practice [1, 2]. In common, these expression profiles derived from the whole tumor tissue, that comprehends both malignant cells, as well as variable proportions of stromal cells.

Breast cancer behavior is a reflection of an interactive signaling between the malignant epithelial compartment and the surrounding microenvironment, composed of stromal cells, including carcinoma associated fibroblasts, mesenchymal stem cells, tumor associated macrophages, endothelial cells, pericytes, adipocytes and lymphocytes, as well as extracellular matrix components [3]. The interaction among these compartments may be mediated by secreted factors, cell-matrix interactions, as well as cell-cell direct contact.

There is evidence that stromal cells of normal tissues behave quite distinctly from stromal cells of tumoral tissues. Normal stroma may inhibit cell proliferation, in contrast with tumor stroma, that may support tumor development and progression, through the induction of cancer cells proliferation, migration and invasion, as well as the activation of angiogenesis [3-5]. There is also evidence that both the extracellular matrix as well as the stromal cells may play a role in drug resistance and disease prognosis [6-8]. In accordance, there are reports indicating that the disorganised stroma is associated with poor response to chemotherapy but in contrast, it is inversely related with lymph node metastases [9]. In addition, it was suggested that a high stromal gene expression, characterizing a reactive stroma, may be associated with resistance to neoadjuvant chemotherapy in estrogen receptor negative tumors [7]. This signature however, was not specifically derived from the stromal tumor compartment itself. Furthermore, in triple negative breast cancer, increased levels of stromal tumor infiltrating lymphocytes were shown to predict pathologic complete response [10]. Eryilmaz et al [2018] [11] showed the importance of stromal and intratumoral tumor lymphocyte infiltration for pathologic complete response in patients with locally advanced breast cancer who received neoadjuvant chemotherapy.

Hence, our aim was to evaluate whether a stromal cell transcriptional signature might be associated with response to neoadjuvant anthracycline and taxane, in locally advanced breast cancer, using a direct approach of stromal cell selection.

2. PATIENTS AND METHODS

This protocol was approved by the Institutional Ethics Committee (Comitê de Ética do Hospital de Câncer de Barretos, protocol number 135/2008; Comitê de Ética para Análise de Projetos de Pesquisa do Hospital das Clínicas da Faculdade de Medicina da Universidade de São Paulo, protocol number 1256/09). A written informed consent was signed by all participants. This study was registered at ClinicalTrials.gov (Identifier NCT00820690).

Inclusion criteria were women with locally advanced breast cancer and clinical conditions to receive treatment with doxorubicin, cyclophosphamide and paclitaxel. Exclusion criteria were patients diagnosed with inflammatory breast cancer or previous treatment for breast cancer.

Neoadjuvant chemotherapy followed the hospital treatment protocol, consisting of 4 cycles of doxorubicin 60 mg/m^2 and cyclophosphamide 600 mg/m^2, every 21 days, followed by 4 cycles of paclitaxel 174 mg/m^2 every 21 days (or 80 mg/m^2 weekly for 12 weeks). Response was defined as pathological complete response (PCR) or downstaging to maximum ypT1a-b/ypN0, after chemotherapy.

2.1. Stromal cell selection and Microarray analysis

Fresh frozen tumor fragments were cut in 10 μm slices and stromal cells were microdissected using CapSure HS LCM (Thermo Fisher Scientific) in a Pix Cell II Arcturus Laser Capture Microdissection (Thermo Fisher Scientific) (LCM) (S1 Figure.). After addition of a lysis solution, total RNA was recovered from a RNA purification column (Arcturus PicoPure RNA isolation, Thermo Fisher Scientific).

Both total RNA extracted from samples and Universal Reference RNA (Stratagene California, La Jolla, CA, USA) were linearly amplified, using two-round RiboAmp HS^{Plus}2-round (Thermo Technologies) and Low Input Quick Amp kit (Agilent Technologies) protocols and labelled with CY5 or CY3, respectively. Samples were analyzed on a NanoDrop spectrometer (Thermo Fisher Scientific) and yield values varied between 0.79 – 5.93 μg of cRNA and specific activity between 6.36 – 10.75 pMol Cy3 or Cy5 per μg cRNA. Competitive hybridization was performed in the SurePrint G3 8×60K slides (Agilent Technologies) and fluorescence intensities from scanned image files in an Agilent Bundle Model B Microarray Scanner System (Agilent Technologies) were pre-processed with Agilent Feature Extraction software (v10.7.1) and normalized using GeneSpring GX12.1 software (Agilent Technologies). A detailed description of methods is provided in Supplementary methods (S methods).

Comparisons of expression levels were performed using MeV (MultiExperiment Viewer, version 4.5.1.) software applying SAM (Significance analysis of microarrays). Analysis was done using all sequences (without filtering). Unsupervised hierarchical clustering based on Euclidean distance and average linkage was used to verify association patterns. The reliability of the clustering was assessed by the Bootstrap technique using MEV. Raw data from microarray was deposited at the Gene Expression Omnibus (GEO).

Classification of stromal samples according to response was also analyzed using the order of medians, based on confidence statements [12,13]. This method compares the median expression of each microarray marker for detection of a difference between the two populations of samples (downstaging vs non-downstaging), and a confidence statement of the difference. With the list of the confidence statements for all markers, pairs of over and under expressed markers are chosen sequentially, based on the highest confidence values. The first pair is chosen as the markers over (O) and under (U) expressed in downstaging (as compared with non-downstaging) samples with the highest confidence; the relation index O/U is calculated for each sample. Afterwards, the confidence statement that median index value for O/U, is greater in downstaging (M1) as compared with non-dowstaging samples (M2), is computed. If the confidence statement is not high enough, the second pair of over and under expressed genes (with the second highest confidence) is added. Then, the product of the two over expressed markers is divided by the product of the two under expressed, for each sample, and a new confidence statement is calculated for M1>M2, and if not high enough, a third pair of markers is added, and so on, until a final index value with a satisfactory confidence is attained for the separation of the two populations of samples (S methods) [12,13].

Gene list enrichment analysis and candidate gene prioritization, based on functional annotations and protein interactions network, was performed using Toppgene suite, with FDR correction p value cut off ≤ 0.05 (https://toppgene.cchmc.org/enrichment.jsp) [14].

Gene set enrichment analysis (GSEA) was used to identify whether predefined gene sets might associate with gene expression differences between phenotypes (available at http://software.broadinstitute.org/gsea/index.jsp). In this pairwise comparison, all genes are ranked based on signal-to-noise ratio. Then, the alternative hypothesis, that rank ordering of distinct pathway members is associated with a specific phenotype, is tested [15]. This methodology makes it possible to detect situations where all genes, in a predefined set, change in a small, but coordinated way. FDR<0.25 was considered significant. Some results assumed FDR < 0.1 or < 0.01, because even using more stringent cut offs, these lists comprehended at least 100 gene sets. GSEA collection was identified by searching google tool for gene set name.

Data derived from gene expression was also investigated for enriched networks, using Ingenuity Pathway Analysis, IPA (Qiagen).

The ROC plotter, an online transcriptome-level validation tool for predictive biomarkers was used to investigate the potential association of 10 highlighted genes with pathological complete response to any chemotherapy [16]. The best performing threshold was used as the cutoff. Also, the genes were analyzed without filters or with filters for adjuvant and neoadjuvant chemotherapy

3. RESULTS

3.1. Patients

Forty four patients diagnosed with locally advanced breast cancer, between July 2008 and January 2012, at Hospital de Câncer de Barretos, Barretos, SP, Brazil, were included. Patients´ median age was 43 years (21-64 y). All patients presented stage III disease and mean tumor dimension pre-chemotherapy was 7.0 cm (± 2.0) and post-chemotherapy was 4,2 cm (± 3.4). All patients, except for three, were diagnosed with invasive ductal carcinoma and among tumors, 29 were classified as ER positive and 15, as ER negative (Table 1). All patients received the recommended neoadjuvant chemotherapy, except for five, who interrupted treatment due to intolerance or lack of tumor reduction. Median time between last cycle of chemotherapy and breast surgery was 35 days. After chemotherapy, nine patients presented disease downstaging to maximum ypT1a-b/ypN0, including four, who presented pathological complete response. After a median follow up of 60 months (9.0–87.0 months), 23 patients presented recurrence of the disease, among whom, 20 patients died due to cancer. Another patient died from a cause other than cancer.

Id	*Age (y)*	*HT*	*ER*	*PR*	*HER2*	*Ki67 (%)*	*T dim preCT (cm)*	*T dim postCT (cm)*	*ypTN (postCT)*
52	≤40	D	+	+	-	5	6.0	3.5	ypT2N0
84	>40	L	+	-	-	5	8.0	0.0	ypT0N0
67	>40	D/L	+	+	-	10	8.3	18.0	ypT4N3
20	≤40	D	+	+	-	10	6.0	6.0	ypT4N2
71	≤40	D/IS	+	+	-	10	7.6	4.5	ypT2N3
66	>40	D	+	+	-	60	11.0	0.8	ypT1bN0
68	>40	D	+	+	-	80	8.0	5.4	ypT3N2

33	>40	D	+	+	-	20	6.0	0.6	ypT1bN2
64	≤40	D	+	+	-	20	8.0	1.8	ypT1cN1
54	>40	D	+	+	-	20	9.0	8.3	ypT3N0
19	>40	D	+	+	-	20	7.0	8.0	ypT3N2
37	≤40	D	+	+	-	20	6.5	6.5	ypT3N1
58	≤40	D	+	-	-	30	10.0	11.0	ypT4N3
7	>40	D	+	+	-	30	7.8	1.5	ypT1cN3
79	≤40	D	+	+	-	70	5.2	0.0	ypT0N0
9	>40	D	-	+	-	70	4.0	4.4	ypT2N0
6	>40	D	-	+	-	80	6.0	7.8	ypT4N2
73	≤40	D	+	+	-	80	8.0	5.8	ypT3N2
63	>40	D	+	+	-	90	6.5	0.6	ypT1bN0
80	≤40	D	+	+	-	90	6.1	2.8	ypT4Nx
81	≤40	D	+	-		100	6.4	5.0	ypT2N1
30	>40	L	+	+	-	ND	6.0	5.5	ypT3N1
56	≤40	D	+	+	+	ND	14.0	6.8	ypT3N1
62	>40	D	+	+	-	10	6.0	2.0	ypT1cN0
55	>40	D	+	+	-	10	5.5	6.3	ypT4N2
99	>40	D	+	+	+	10	12.0	0.8	ypT4N0
17	>40	D	+	-	+	20	8.0	9.0	ypT4N2
69	≤40	D	+	-	-	90	5.5	9.0	ypT3N3
18	>40	D	+	-	-	90	4.0	1.7	ypT1N2
11	>40	D	+	+	+	ND	7.0	2.2	ypT2N2
72	>40	D	+	+	+	ND	5.5	0.0	ypT0N1
59	>40	D	-	-	+	60	6.0	5.8	ypT3N1
49	>40	D	-	-	+	90	8.0	0.0	ypT1miN0
60	≤40	D	-	-	-	ND	3.5	0.0	ypT0N0
44	≤40	D	-	-	+	100	5.4	2.0	ypT1cN0
70	>40	D/O	-	-	-	40	5.1	4.5	ypT2N2
75	>40	D	-	-	-	60	7.0	7.5	ypT4N3
51	≤40	D	-	-		80	8.9	4.5	ypT4N1
38	>40	D	-	-	-	90	5.2	1.0	ypT1bN0
36	≤40	D	-	-	-	90	6.5	4.0	ypT4N3
76	>40	D	-	-	-	90	8.5	0.0	ypTisN0
45	>40	L	-	-	-	ND	7.5	4.0	ypT4N3
13	≤40	D	-	-	-	ND	6.5	4.2	ypT2N1
61	>40	D	-	-	-	100	5.5	0.3	ypT1aN0

Table 1. Abbreviations: HT: histological type: ductal (D); lobular (L); other (O); IS (in situ); Tdim: Tumor dimension, preCT and postCT (chemotherapy); T1mi: T1 microscopic; (-): negative; (+): positive. ER and PR were considered positive if ≥ 1% malignant cells were stained. ND: not done.

3.2. Stromal cells transcriptional profile

At first, we evaluated whether information on tumoral estrogen receptor status, determined through immunohistochemistry of malignant cells, would classify the microdissected stromal cells. Using SAM test (FDR zero), 51 sequences were differentially expressed, 32 more expressed in stromal cells from ER positive (including *ESR1*, *GATA3*, *NAT1*, *TFF3*) and 19 more

181 expressed in ER negative samples (S1 Table). Unsupervised hierarchical clustering and
182 bootstrapping, using these sequences, could separate samples in two branches, one of them
183 including all 29 ER positive (by immunohistochemistry) and the other including 13/15 ER
184 negative samples (Figure. 1), resulting in 95.4% accuracy. Gene list enrichment through Toppgene
185 Suite analysis, included "genes up regulated in breast cancer samples positive for ESR1
186 compared to the ESR1 negative tumors" such as: *ABAT*, *ANXA9*, *DACH1*, *DNALI1*, *ERBB4*, *ESR1*,
187 *EVL*, *GATA3*, *GREB1*, *NAT1*, *RET*, *SYT1*, *TFF3*.

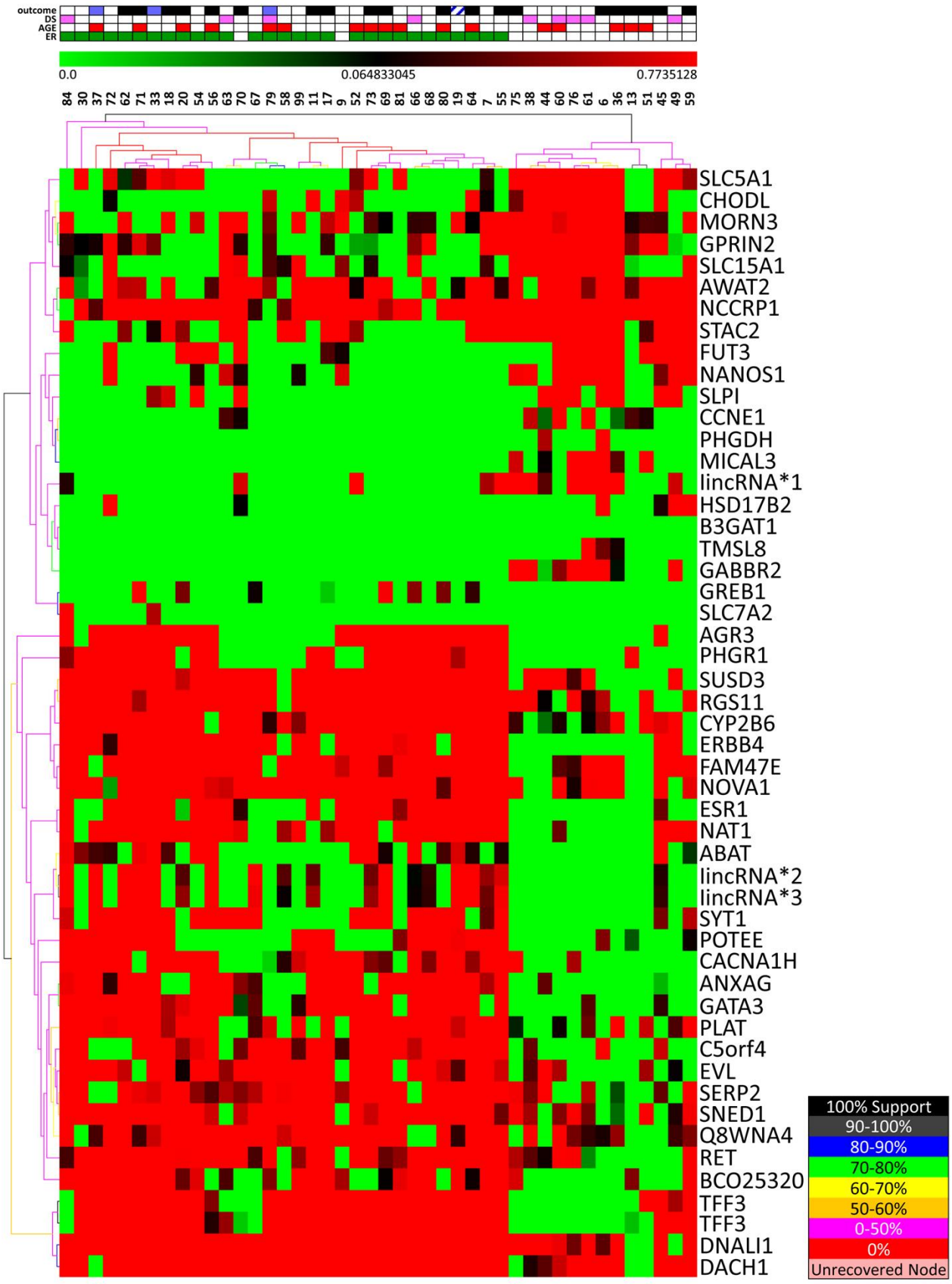
outcome
DS
AGE
ER
0.0
0.064833045
0.7735128
84 30 37 72 62 71 33 18 20 54 56 63 70 67 79 58 99 11 17 9 52 73 69 81 66 68 80 19 64 7 55 75 38 44 60 76 61 6 36 13 51 45 49 59
SLC5A1
CHODL
MORN3
GPRIN2
SLC15A1
AWAT2
NCCRP1
STAC2
FUT3
NANOS1
SLPI
CCNE1
PHGDH
MICAL3
lincRNA*1
HSD17B2
B3GAT1
TMSL8
GABBR2
GREB1
SLC7A2
AGR3
PHGR1
SUSD3
RGS11
CYP2B6
ERBB4
FAM47E
NOVA1
ESR1
NAT1
ABAT
lincRNA*2
lincRNA*3
SYT1
POTEE
CACNA1H
ANXAG
GATA3
PLAT
C5orf4
EVL
SERP2
SNED1
Q8WNA4
RET
BCO25320
TFF3
TFF3
DNALI1
DACH1
100% Support
90-100%
80-90%
70-80%
60-70%
50-60%
0-50%
0%
Unrecovered Node

Figure. 1. Unsupervised hierarchical clustering of stromal cells microdissected from tumors categorized according estrogen receptor status, as determined by immunohistochemistry, in positive (upper panel in green) or negative. Estrogen receptor (ER) and progesterone receptor (PR) expression in malignant cells were evaluated using anti-estrogen receptor alpha rabbit monoclonal antibody SP1 (Thermo Fisher Scientific, Walthan, MA, USA) and CONFIRM anti-progesterone receptor rabbit monoclonal antibody (Roche AB, Christian Sundberg, Stockholm, Sweden), respectively, and were considered positive if ≥ 1% malignant cells were stained. Stromal cells were microdissected from samples. Gene expression profile was determined using Agilent platform and 51 sequences were found differentially expressed. Each column represents one tumor sample and each line represents the expression of one sequence: green less expressed; red: more expressed. Gene symbol appears on the right. Lines on the top of the dendogram: black, blue, green: high confidence; yellow and pink: low confidence (color scale in accordance to support is represented in the box, on the right). Characteristics of patients and tumor samples appear on the upper box: outcome (blue: alive with disease recurrence; black: deceased): age (red: ≤ 40y); ER (immunohistochemistry: green, positive); DS (downstaging: pink, yes). Green - red scale bar on the top: ER positive/ER negative.

We have then evaluated whether information on the age of the patients, categorized as ≤40 (young adults) and > 40 years, would classify the microdissected stromal cells. A differential gene expression profile, according to patients´ age, included 30 sequences (SAM, FDR 10) (S2 Table), all of which were more expressed in patients older than 40. Hierarchical clustering, using this gene expression profile, correctly classified 93.1% of the samples (S2 Figure.), however, no gene ontology categories, enriched in these differentially expressed genes, were identified (http://toppgene.cchmc.org/enrichment.jsp).

Our next aim was to identify a differential gene expression profile, considering tumor down staging (to at least ypT1a/b,ypN0), as the best response. Using SAM test (FDR 17), 11 sequences (including nine genes) were differentially expressed, all of which (except for *H2AFJ*) more expressed in responsive tumors, from patients who presented tumor down staging (S3 Table). These sequences could correctly classify 93.1% of the samples, with high confidence, using unsupervised hierarchical clustering and bootstrapping (Figure. 2). Gene list enrichment analysis revealed three genes involved in "abnormal cytotoxic T cell physiology (mouse phenotype)": *TOX*, *LY75* and *SH2D1A* (http://toppgene.cchmc.org/enrichment.jsp). In addition, Ingenuity Pathway Analysis, IPA, revealed that "Cancer" was a network enriched in the gene list (S3 Figure).

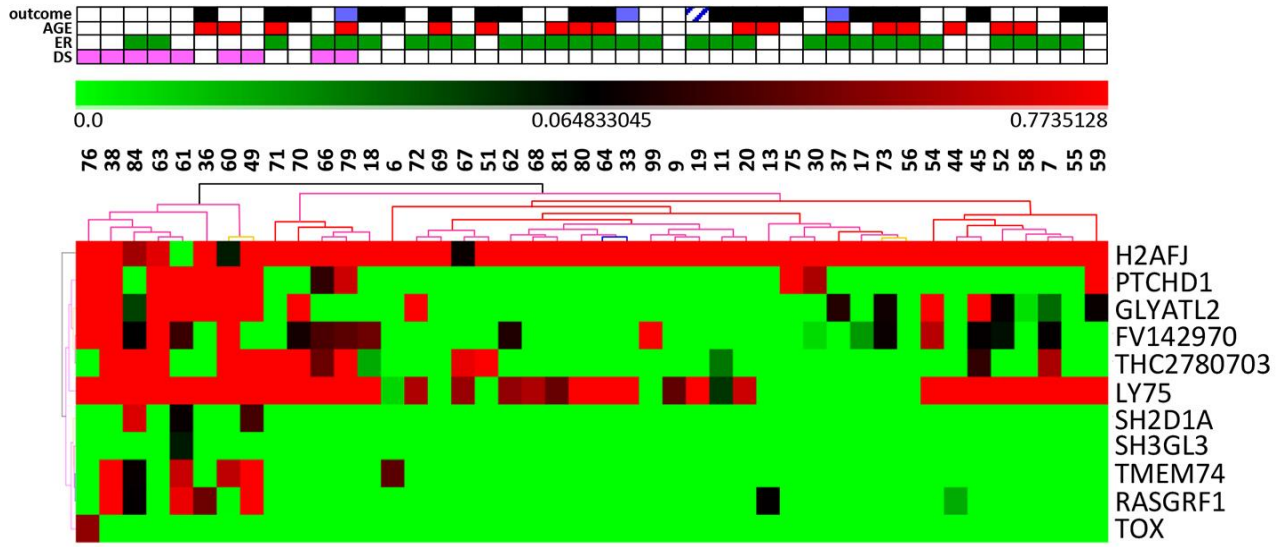

Figure 2. Unsupervised hierarchical clustering of stromal cells from tumors categorized as DS (Down Staging) and NDS (Non Down Staging). Stromal cells were microdissected from samples. Gene expression profile was determined using SurePrint G3 Microarray, Agilent, applying SAM test (FDR 17) and 11 sequences were found differentially expressed. Unsupervised hierarchical clustering and bootstrapping, using these sequences, identified two branches with high confidence, one including 9/44 down staging (responsive in pink, upper box) samples and the other including all non-down staging (non-responsive) samples and one responsive sample, as well. Green - red scale bar on the top: DS/NDS

To further evaluate genes that might classify samples according to tumor response we have used another statistical method, the order of median based on confidence statements. This method allows the identification of pairs of markers that may classify downstaging vs non-downstaging samples. At first, median expression for each microarray marker was compared in downstaging vs non-downstaging samples and the confidence of difference between medians was computed. With a list of 446 microrarray markers with confidence statements > 0.95, over and under expressed pairs of markers in downstaging samples, based on the highest confidence statements, were chosen sequentially, and the relation between them was calculated for each sample. For our data set, we could stop at the following 4 pairs of markers that were over and underexpressed, respectively, in downstaging samples: *PTCHD1/PDXDC2P; LOC100506731/NEURL4*; *SH2D1A/ENST00000478672; TOX/H2AFJ.* The final index, representing the product of the relation of these four pairs of markers, could separate each tumor sample, according to response to neoadjuvant chemotherapy, and values appear on Figure. 3. This final index allowed us to state that the confidence that the median value in downstaging sample was greater than in non-downstaging samples, $Mi_1 > Mi_2$ was 99.8.

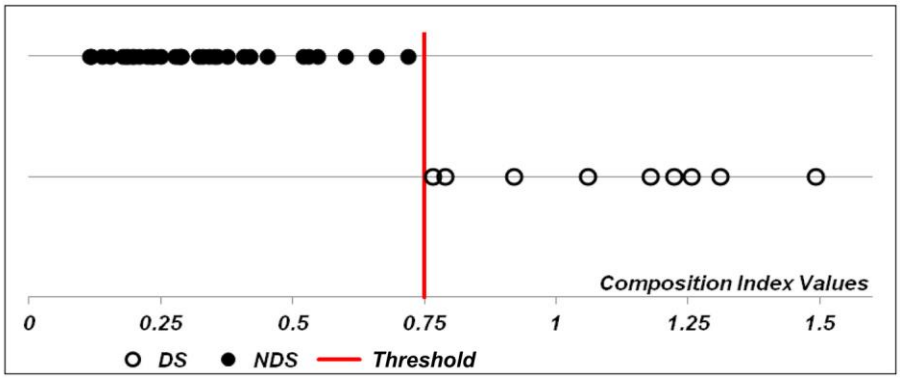

Figure 3. Classification of stromal cells samples according to tumor response (downstaging, DS, vs non-downstaging, NDS) according to the order of median based on confidence statements. Sample classification was based on the composition index value, calculated as the product of the relation of pairs of genes overexpressed and underexpressed in downstaging samples: PTCHD1 and PDXDC2P; LOC100506731 and NEURL4; SH2D1A and ENST00000478672; TOX and H2AFJ. The red line represents the threshold to classify samples in one of the two populations.

Moreover, we have evaluated the predictive potential of our main candidates, using ROC plotter, an on line tool that allows assessment to publicly available transcriptomic results of a large set of breast cancer patients submitted to neoadjuvant chemotherapy, that includes: taxane, anthracycline, ixabepilone, CMF, FAC and FEC. Interestingly, all the three genes involved in "abnormal cytotoxic T cell physiology (mouse phenotype)": *TOX*, *LY75* and *SH2D1A*, were more expressed in responsive samples, confirming our results (Figure 4). However, *PTCHD1*, *H2AFJ* and *NEURL4* were not differentially expressed in this set of samples.

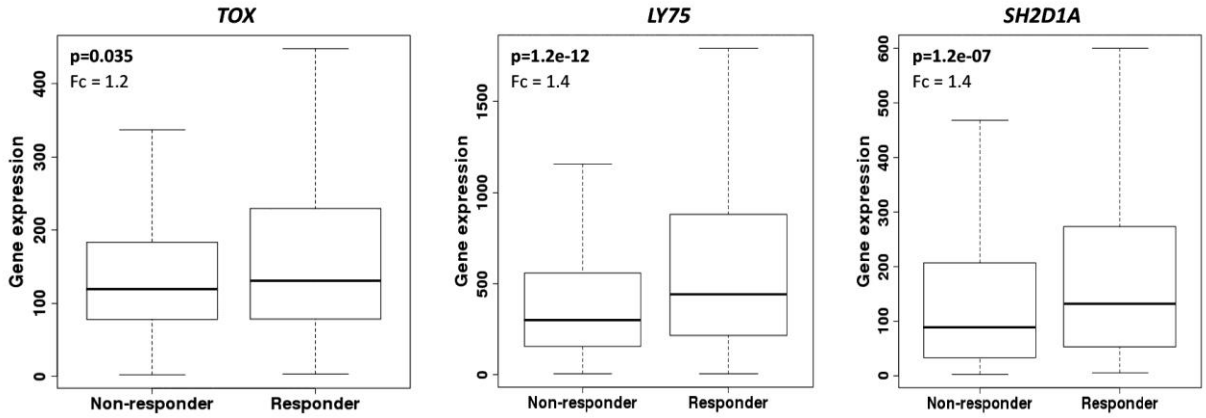

Figure 4. Expression of biomarkers according to pathological complete response to any chemotherapy in 1632 samples from breast cancer patients (1100 non-responders; 532 responders). ROC plotter (Fekete et al., 2019 [16]). p: Mann Whitney test. Fc: fold change.Probes used for TOX: 204529_s_at; Ly75: 205668_at; SH2D1A: 210116_at

Our next step was to use GSEA to identify gene sets that might be correlated with the phenotype downstaging or with the phenotype non-downstaging. Considering gene expression derived from all 44 tumor samples, GSEA revealed 117 gene sets correlated with tumor

281 downstaging (FDR < 0.01), including 7 KEGG gene sets, comprehending two immune system
282 related gene sets (antigen processing and presentation; T cell receptor signaling pathway), as well
283 as 15 GO biological process gene sets among which, at least 10, involved with immune response,
284 including five implicated in induction or activation of this process: positive regulation of
285 lymphocyte activation, positive regulation of immune system process, positive regulation of T
286 cell activation, T cell activation, lymphocyte activation (Table 2; S4 Table.). In addition, GSEA
287 revealed 23 gene sets correlated with tumor non-downstaging (FDR < 0.25), among which, no
288 gene sets cataloged in the KEGG pathway database and only one cataloged in the GO gene set
289 cellular component (synaptic vesicle) (S5 Table).
290

GO gene sets (biological process)	Genes (CORE ENRICHMENT)
ADAPTIVE_IMMUNE_RESPONSE_GO_0002460	FOXP3 CD74 CRTAM C2 TRAF2 MAP3K7 TNFSF13 SOCS5 TRAF6 IL18 TLR8 EBI3 PTPRC CD40LG
ADAPTIVE_IMMUNE_RESPONSE	FOXP3 CD74 CRTAM C2 TRAF2 MAP3K7 TNFSF13 SOCS5 TRAF6 IL18 BCL10 TLR8 EBI3 PTPRC CD40LG
POSITIVE_REGULATION_OF_LYMPHOCYTE_ACTIVATION	CD47 LCK NCK1 CD24 CD3E ICOSLG TNFSF13 ZAP70 SOCS5 IL18 EBI3 PTPRC SIRPG
REGULATION_OF_IMMUNE_SYSTEM_PROCESS	FOXP3 APOBEC3G CD47 LCK TGFB2 NCK1 LAX1 CD24 CD3E ICOSLG CRTAM C2 TRAF2 MAP3K7 TNFSF13 ZAP70 SOCS5 TRAT1 TRAF6 IL18 EREG UBE2N TLR8 EBI3 PTPRC SIRPG NCR1 FYN NFAM1 LAT2 INHBA CD28
POSITIVE_REGULATION_OF_IMMUNE_SYSTEM_PROCESS	CD47 LCK TGFB2 NCK1 CD24 CD3E ICOSLG CRTAM C2 TRAF2 MAP3K7 TNFSF13 ZAP70 SOCS5 TRAT1 TRAF6 IL18 EREG UBE2N TLR8 EBI3 PTPRC SIRPG FYN NFAM1 LAT2 CD28
POSITIVE_REGULATION_OF_T_CELL_ACTIVATION	CD47 LCK NCK1 CD24 CD3E ICOSLG ZAP70 SOCS5 IL18 EBI3 PTPRC SIRPG
IMMUNE_RESPONSE	LY75 FOXP3 APOBEC3G IL15 CTSS TRIM22 TLR7 PTGER4 POU2AF1 PRKRA CD74 TGFB2 IL10RB DEFB1 TAPBP LAX1 CXCL13 HLA-DRB3 FYB BLNK NFIL3 CD96 SKAP1 CRTAM C2 TRAF2 IRF8 CD83 CTSC TCF7 MAP3K7 TNFSF13 CHUK ZAP70 IL2 YTHDF2 SOCS5 TRAT1 CCL5 TRAF6 IL6 AIM2 IL18 CCL25 BCL10 IKBKAP EREG LCP2 CXCR4 OPRK1 UBE2N CCL20 TNFAIP1 CCL2 LTB4R TLR8 CEBPB WAS CD164 SECTM1 GTPBP1 EBI3 CD7 TCF12 CD79B IL2RG GEM PTPRC GZMA CCR5 NCR1 CCL23 GPR65 FYN CD40LG XBP1 DPP4 CCR2 MAP4K2 APOA1 NFAM1 NCF4 LAT2
_S_TRANSITION_OF_MITOTIC_CELL_CYCLE	CUL2 CUL1 GFI1 CDKN2A LATS2 CDKN2C PPP6C ACVR1 CDKN1B INHBA CDCA5 CDKN1A GSPT1 ACVR1B CDKN2D RCC1
DNA_DEPENDENT_DNA_REPLICATION	GTPBP4 MSH5 RFC4 RAD17 CCDC88A RFC3 MSH6 MSH2 PRIM1 POLA1 TSPYL2 RFC1 PRIM2 GMNN POLB EREG HMGB2 CDK2AP1 REV3L S100A11 EXO1 NBN CDC6 MLH1 RPAIN

T_CELL_ACTIVATION	FOXP3 CD47 LCK NLRC3 NCK1 LAX1 CD24 CD3E ICOSLG CRTAM NHEJ1 ZAP70 IL2 SOCS5 IL18 EBI3 CD7 PTPRC SIRPG
APOPTOSIS (APOPTOSIS_GO)	CASP1 BAX NFKB1 IRF1 TNFRSF21 IRF4 GZMB FAS BID NFKBIA CASP3 TRAF2 CASP7 CHUK BIRC2 MDM2 TP53 TRAF3 TNF NFKBIE FASLG CASP4 APAF1 BIRC3 CASP6 TRAF1 CYCS
REGULATION_OF_IMMUNE_EFFECTOR_PROCESS	FOXP3 APOBEC3G CRTAM TRAF2 MAP3K7 TRAF6 PTPRC NCR1
LYMPHOCYTE_ACTIVATION	FOXP3 CD47 LCK NLRC3 NCK1 LAX1 CD24 CD3E ICOSLG CRTAM TPD52 NHEJ1 TNFSF13 ZAP70 IL2 SOCS5 IL18 EBI3 CD7 PTPRC SIRPG CD40LG NFAM1 LAT2 INHBA CD28 CD3D
POSITIVE_REGULATION_OF_CYTOKINE_PRODUCTION	TRAF2 NOD2 MAP3K7 TRAF6 EREG IFNG ATP6AP2 CD40LG
POSITIVE_REGULATION_OF_MULTICELLULAR_ORGANISMAL_PROCESS	CD47 LCK TGFB2 NCK1 CD24 CD3E ICOSLG CRTAM C2 TRAF2 NOD2 MAP3K7 TNFSF13 ZAP70 SOCS5 TRAT1 TRAF6 IL18 EREG IFNG UBE2N TLR8 EBI3 PTPRC ATP6AP2 SIRPG BMP4 FYN CD40LG NFAM1 LAT2 CD28 MC4R

Table 2. Gene expression of all 44 stromal cell samples were analyzed through GSEA (gene set enrichment analysis) (FDR < 0.01). Gene sets and rank ordering of distinct pathway members, associated with the phenotype downstaging, are shown.

We have also used GSEA to identify gene sets correlated with tumor response specifically in ER positive tumors, as well as in ER negative tumors, separately.

In ER positive tumors, GSEA revealed 214 gene sets (FDR <0.25) correlated with tumor downstaging (S6 Table.). Using a more stringent FDR value (< 0.1), tumor down staging was correlated with one KEGG gene set: antigen processing antigen presentation (comprehending *CD74*, *CD8A*, *CD8B*, and 9 molecules of HLA complex, among others) and four GO gene sets (biological process), including one related with immune response: regulation of T cell activation (comprehending genes such as *ZAP70*, *LCK*, *CD24*, *CD47*, *CD3E*, among others).

In ER negative samples, GSEA identified 998 gene sets, using FDR < 0.25, that were correlated with tumor downstaging. Using a more stringent FDR cut off (< 0.05), five KEGG gene sets were correlated with tumor downstaging, including two related with immune response: antigen processing and presentation and T cell receptor signaling pathway, as well as at least 12 GO gene sets (biological process) related with the immune process, including two, with FDR < 0.01, which were adaptive immune response and positive regulation of T cell activation (S7 Table.).

In ER positive samples that did not present tumor down staging, 49 gene sets were found in GSEA analysis (FDR < 0.25), including one KEGG gene set: ECM receptor interaction (including 5 types of integrins, 6 collagens, 4 laminins, fibronectin 1 and trombospondin 1); eight GO gene sets (biological process): cell adhesion; cell recognition; embryonic development; (cellular component): cortical cytoskeleton; cell projection part; cell surface; cytosolic part; (molecular function): oxidoreductase activity (S8 Table.).

In ER negative tumors that did not present downstaging, 39 gene sets were identified in GSEA analysis (FDR < 0.25), including two KEGG pathways, related with arginine and proline metabolism as well as four GO gene sets (FDR < 0.1) (cellular component): intermediate filament cytoskeleton (including *KRT6A*, *KRT1*, *KRT19*, *KRT18*, *KRT31*), synaptic vesicle and intermediate filament; (molecular function): neuropeptide receptor activity (S9 Table).

In estrogen receptor negative tumors, a 50-gene signature [7], reflecting the activation state of the tumor stroma, was previously described as a predictor of poor response, that was characterized as non-pathological complete response to anthracycline based chemotherapy. We have then used this list of genes to perform a hierarchical clustering analysis of 15 ER negative samples. Expression of these 50 genes, however, could not correctly classify samples according to response to chemotherapy, as it was rather homogeneous and most samples presented a relatively high expression of a group of genes, including FAP, fibroblast activation protein, alpha; three types of collagen, *COL3A1*, *COL10A1*, *COL5A2*; two metalloproteases, *MMP11* and *MMP14*, among seven others. In addition, most samples presented a relatively moderate/high expression of *PRSS11* (or *HTRA1*, HtrA serine peptidase 1), *COL1A2*, *MMP2*, *TGFB3*, *SPARC* and *DCN* (decorin), as well as a relatively low expression of another group of genes, including *SNAI2* and *THBS2* (S4 Figure.).

Finally, we searched our samples for a gene profile that might differentiate the stromal cells, according to disease outcome, defined as recurrence of disease or death, however, we could not identify a stromal prognostic signature. We have also tested whether a previously identified stromal gene profile, associated with disease outcome, named stroma-derived prognostic predictor, SDPP [6], could predict recurrence or death of our patients. The expression of 24 genes, out of the whole list of 26 genes described in SDPP (excluding *TRBV5-4* and *C21orf34*, which were not tested in our samples), however, could not cluster the samples, according to disease outcome (S5 Figure).

4. DISCUSSION

We have directly analyzed breast cancer stromal cells to identify a predictive signature of response to neoadjuvant chemotherapy. Using microdissected stromal cells we could identify eight genes more expressed in tumors presenting downstaging, including three genes involved in abnormal cytotoxic T cell physiology, such as *TOX*, *LY75* and *SH2D1A*. In addition, gene sets correlated with tumor downstaging were mainly related with immune system pathways.

In our study, genes, such as *GATA3*, *ERBB4*, *RET*, *NAT1*, *TFF3*, typically more expressed in ER positive tumor samples, were also more expressed in stromal cells from ER positive compared to ER negative tumors (defined by immunohistochemistry of malignant cells) [17-19. This result may reflect estrogen responsiveness, mediated by ER expression in stromal fibroblasts [20], as well as some degree of contamination of the samples of microdissected stromal cells with malignant cells (ER positive or ER negative). Among genes more expressed in ER negative tumors was *HSD17B2*, which codes an enzyme involved in metabolizing androgens and estrogen to less active metabolites, further indicating that the estrogen pathway is not critical in these tumors.

We could identify a panel of differentially expressed genes between young (less than 41 years) and older patients. This was rather expected because differences in expression levels of dermal fibroblast from young and old human beings were already described [21]. In addition, menopause is associated with senile involution of the breasts, characterized by progressive changes in the assemblage of the mammary parenchyma and reduced breast density, reflecting stroma and adipose tissue replacement of the alveoli [22]. However, in the present group of

samples, we could not identify gene sets associated with particular pathways, neither identify a differential profile using higher age cutoffs of 45 and 50 years (data not shown).

In stromal cells from responsive tumors, genes such as *PTCHD1*, *LY75*, *SH2D1A* and *TOX*, were more expressed, while *H2AFJ* was less expressed. More interestingly, a group of 4 pairs of genes were sufficient to classify samples according to response, *PTCHD1*/*PDXDC2P*; *LOC100506731*/*NEURL4*; *SH2D1A*/*ENST00000478672*; *TOX*/*H2AFJ* with a high confidence.

H2AFJ encodes a member of the histone H2A super family, that may be overexpressed in breast cancer samples through gene amplification, and considered a putative breast cancer oncogene [23]. Consistent with the observed *H2AFJ* overexpression in non responsive breast cancer samples, in colorectal cancer cell lines, *H2AFJ* was described as a mediator of chemoradiation resistance (Wang et al., 2019) [24].*PTCHD1* codes a patched-related protein, structurally similar to the Hedgehog (Hh) receptors PTCH1 and PTCH2. PTCHD1 exhibits biochemical activity in Hh-dependent processes similar to the inhibitory effect of PTCH1 and PTCH2 on Gli-dependent transcription and may be expressed in mammary glands [25]. PTCH1 directly inhibits Smoothened (SMO) and in a mouse model of pancreatic cancer, SMO inhibition may facilitate chemotherapy delivery and extend survival by depleting tumor-associated stromal tissue [26]. This mechanism might also be involved in chemotherapy induced down staging in breast cancer samples.

SH2D1A and *TOX* were previously shown to be up regulated in germinal center T helper cells compared to other CD4+ T-cell subsets [27]. However, TOX overexpression in CD8+ tumor-infiltrating lymphocytes was also related with tumor immunosuppressive microenvironment, T cell exhaustion and tumor persistence (Scott et al., 2019) [28]. In turn, *LY75 (CD205)* is expressed at relatively high levels on myeloid blood dendritic cells and monocytes and plays a role in endocytic uptake of antigen and presentation to lymphocytes via MHC class II molecules [29, 30]. The present results may reveal that a complex interrelationship among specific players of the immune response take place in responsive tumors to AC-T.

In addition, various immune response gene sets were positively correlated with tumor downstaging. These gene sets comprehended genes such as *CD24*, that modulates B-cell activation responses, *CD3D* and *CD3E*, which are part of the T-cell receptor/CD3 complex, that couples antigen recognition to several intracellular signal-transduction pathways; *CD7*, found on thymocytes and mature T cells and playing an essential role in T-cell interactions; *CD40LGT*, expressed on the surface of T cells, regulating B cell function by engaging CD40 on the B cell surface; *CD74*, that associates with class II major histocompatibility complex (MHC) and is an important chaperone that regulates antigen presentation for immune response; *CD79B*, the B lymphocyte antigen receptor, a multimeric complex that includes the antigen-specific component, surface immunoglobulin (Ig), necessary for expression and function of the B-cell antigen receptor; *CD83*, involved in the regulation of antigen presentation; CD96, that plays a role in the adhesive interactions of activated T and NK cells during the late phase of the immune response, as well as function in antigen presentation.

Interestingly, gene sets enriched in immune related genes were more strongly correlated with tumor downstaging in ER negative tumors (more stringent FDR q-values). In accordance, it was previously shown in a cohort of triple negative tumors and HER2 positive tumors, that an increased percentage of stromal T infiltrating lymphocytes, as well as expression of immune activating and immunossupressive genes, are positively correlated to response to neoadjuvant chemotherapy [10]. In our study, immune response gene sets were also correlated with tumor downstaging in ER positive tumors, such as "KEGG antigen processing and presentation", containing genes such as *CD74*, *CD8A*, *CD8B*, and various genes of the HLA complex, as well as

GO biological process gene set such as "regulation of T cell activation", comprehending *ZAP70*, *CD24*, *CD3E*, *LCK*, *IL21*, among others.

There was not a clear pattern of gene sets associated with tumor resistance. However, stromal cells from both ER positive as well as ER negative tumors, which were enriched in cytoskeleton transcripts, might be associated with tumor non-downstaging. In addition, in ER positive tumors, cell adhesion as well as KEGG ECM receptor interaction, might also be involved in tumor resistance.

In the group of estrogen receptor negative samples, we evaluated whether a previously reported stroma-related gene signature would predict resistance [7]. In the present series of microdissected stromal cells however, this gene profile could not separate resistant from responsive samples (pathological complete response or tumor downstaging), and a common pattern of gene expression could be distinguished. A high expression of various collagens and metalloproteases confirm the mesenchymal origin of these samples, whereas expression of *FAP*, a serine protease, indicates the reactive nature of the nontransformed tumor stroma. In a previous work we found that *PRSS11* was more expressed in responsive tumors to doxorubicin based chemotherapy, however, in stromal cells from the current ER negative tumors, it was not differentially expressed between responsive and resistant samples [2].

We could neither detect a stromal signature associated with prognosis in our whole series of samples. In addition, using a previously reported prognostic stromal cell signature identified in ER negative samples, named stroma-derived prognostic predictor, SDPP, we could not predict clinical outcome for patients bearing ER negative tumors in the present series [6]. It is interesting to observe that in the previous study, tumor stroma samples from the good-outcome cluster overexpressed a distinct set of immune-related genes. In the present series of stromal cells, however, gene sets of immune-related genes were mainly correlated with tumor downstaging.

Strengths of our study include the specific evaluation of microdissected stromal cells from patients with locally advanced breast cancer, who underwent the same neoadjuvant chemotherapy regimen and the identification of pairs of genes that might classify tumors according to response to neoadjuvant chemotherapy; limitations include a relatively small number of patients and the intensive labor associated with tumor microdissection, that complicates the use in the clinical practice.

5. CONCLUSION

In summary, tumor stromal cells, which are nontransformed cells, represent an interesting option to evaluate response to neoadjuvant chemotherapy. In locally advanced breast cancer, stromal cells may present specific features of immune response that may be associated with chemotherapy response.

Author Contributions: Conceptualization, M.A.A.K.F., and R.A.C.V.; Data curation, M.L.H.K., and P.A.M.P.S.; formal analysis, M.L.H.K., A.P.C., and C.A.B.P.; Funding acquisition, M.A.A.K.F. and M.M.B.; investigation, M.L.H.K., V.P.A., R.A.R., L.G.C.A.L., and P.A.M.P.S.; methodology, M.A.A.K.F., M.L.H.K., V.P.A., and R.A.R.; Project administration, M.A.A.K.F and R.A.C.V; Resources, M.L.H.K., R.A.C.V., L.M.K., R.A.R., G.E., and S.M.; supervision,M.A.A.K.F.; and M.M.B.; visualization, M.A.A.K.F., M.L.H.K., R.A.C.V., A.P.C., and P.A.M.P.S.; writing—original draft, M.A.A.K.F. and M.L.H.K.; writing—review and editing, M.A.A.K.F. .

Acknowledgments: The authors are very grateful to Mrs. Maria Cristina Piñeiro Grandal, for editing the figures and Conselho Nacional de Desenvolvimento Científico e Tecnológico (CNPq) for support for MAAKF and MMB.

This work was supported by FAPESP 2009/10088-7.

Conflicts of Interest: The authors declare no conflicts of interest.

REFERENCES

1 Chang J.C., Wooten E.C., Tsimelzon A., Hilsenbeck S.G., Gutierrez M.C., Elledge R., Mohsin S., Osborne C.K., Chamness G.C., Allred D.C., et al. Gene expression profiling for the prediction of therapeutic response to docetaxel in patients with breast cancer. Lancet. 2003;362:362-369.

2 Folgueira M.A., Carraro D.M., Brentani H., Patrão D.F., Barbosa E.M., Netto M.M., Caldeira J.R., Katayama M.L., Soares F.A., Oliveira C.T., Reis L.F., Kaiano J.H., Camargo L.P., Vêncio R.Z., Snitcovsky I.M., Makdissi F.B., e Silva P.J., Góes J.C., Brentani M.M. Gene expression profile associated with response to doxorubicin-based therapy in breast cancer. Clin Cancer Res. 2005; 11:7434-7443.

3 Dittmer J, Leyh B. The impact of tumor stroma on drug response in breast cancer. Semin Cancer Biol. 2015;31:3-15.

4 Rozenchan P.B., Carraro D.M., Brentani H., de Carvalho Mota L.D, Bastos E.P, Ferreira E.N., Torres C.H., Katayama M.L., Roela R.A., Lyra E.C., et al. Reciprocal changes in gene expression profiles of cocultured breast epithelial cells and primary fibroblasts. Int J Cancer. 2009;125:2767-2777. doi: 10.1002/ijc.24646.

5 Santos R.P., Benvenuti T.T., Honda S.T., Del Valle P.R., Katayama M.L., Brentani H.P., Carraro D.M., Rozenchan P.B., Brentani M.M., de Lyra EC, et al. Influence of the interaction between nodal fibroblast and breast cancer cells on gene expression. Tumour Biol. 2011; 32:145-157. doi: 10.1007/s13277-010-0108-7.

6 Finak G., Bertos N., Pepin F., Sadekova S., Souleimanova M., Zhao H., Chen H., Omeroglu G., Meterissian S., Omeroglu A., et al. Stromal gene expression predicts clinical outcome in breast cancer. Nat Med. 2008;14:518-527. doi: 10.1038/nm1764.

7 Farmer P., Bonnefoi H., Anderle P., Cameron D., Wirapati P., Becette V., André S., Piccart M., Campone M., Brain E., et al. A stroma-related gene signature predicts resistance to neoadjuvant chemotherapy in breast cancer. Nat Med. 2009;15:68-74. doi: 10.1038/nm.1908.

8 Nakasone E.S., Askautrud H.A., Kees T., Park J.H., Plaks V., Ewald A.J., Fein M., Rasch M.G., Tan Y.X., Qiu J., et al. Imaging tumor-stroma interactions during chemotherapy reveals contributions of the microenvironment to resistance. Cancer Cell. 2012;21:488-503. doi: 10.1016/j.ccr.2012.02.017.

9 Dekker T.J., Charehbili A., Smit V.T., ten Dijke P., Kranenbarg E.M., van de Velde C.J., Nortier J.W., Tollenaar R.A., Mesker W.E., Kroep J.R. Disorganised stroma determined on pre-treatment breast cancer biopsies is associated with poor response to neoadjuvant chemotherapy: Results from the NEOZOTAC trial. Mol Oncol. 2015;9:1120-1128. doi: 10.1016/j.molonc.2015.02.001.

10 Denkert C., von Minckwitz G., Brase J.C., Sinn B.V., Gade S., Kronenwett R., Pfitzner B.M., Salat C., Loi S., Schmitt W.D., et al. Tumor-infiltrating lymphocytes and response to neoadjuvant chemotherapy with or without carboplatin in human epidermal growth factor receptor 2-positive and triple-negative primary breast cancers. J Clin Oncol. 2015;33:983-91. doi: 10.1200/JCO.2014.58.1967.

11 Eryilmaz M.K., Mutlu H., Ünal B., Salim D.K., Musri F.Y., Coşkun H.Ş. The importance of stromal and intratumoral tumor lymphocyte infiltration for pathologic complete response in patients with locally advanced breast cancer. J Cancer Res Ther. 2018; 14: 619-624. doi: 10.4103/0973-1482.174550.

12 Campos C.P., Pereira C.A.B., Rancoita P.M.V., Polpo A. Ordering Quantiles through Confidence Statements. Entropy. 2016, 18: 1-14. doi.org/10.3390/e18100357

13 Marques-F., Paulo C., Pereira, C., A., B. Predictive Analysis of Microarray Data. Open Journal of Genetics. 2014;4: 63-68

14 Chen J., Bardes E.E., Aronow B.J., Jegga A.G. ToppGene Suite for gene list enrichment analysis and candidate gene prioritization. Nucleic Acids Res. 2009;W305-11.

15 Subramanian A., Tamayo P., Mootha V.K., Mukherjee S., Ebert B.L., Gillette M.A., Paulovich A., Pomeroy S.L., Golub T.R., Lander E.S., et al. Gene set enrichment analysis: a knowledge-based approach for interpreting genome-wide expression profiles. Proc Natl Acad Sci U S A. 2005;102:15545-15550.

16 Fekete J.T., Győrffy B. ROCplot.org: Validating predictive biomarkers of chemotherapy/hormonal therapy/anti-HER2 therapy using transcriptomic data of 3,104 breast cancer patients. Int J Cancer. 201924. doi: 10.1002/ijc.32369. [Epub ahead of print] PubMed PMID: 31020993.

17 Doane A.S., Danso M., Lal P., Donaton M., Zhang L., Hudis C., Gerald W.L. An estrogen receptor-negative breast cancer subset characterized by a hormonally regulated transcriptional program and response to androgen. Oncogene. 2006;25(28):3994-4008.

18 Tozlu S., Girault I., Vacher S., Vendrell J., Andrieu C., Spyratos F., Cohen P., Lidereau R., Bieche I. Identification of novel genes that co-cluster with estrogen receptor alpha in breast tumor biopsy specimens, using a large-scale real-time reverse transcription-PCR approach. Endocr Relat Cancer. 2006;13:1109-1120.

19 Yang F., Foekens J.A., Yu J., Sieuwerts A.M., Timmermans M., Klijn J.G., Atkins D., Wang Y., Jiang Y. Laser microdissection and microarray analysis of breast tumors reveal ER-alpha related genes and pathways. Oncogene. 2006; 25:1413-1419.

20 Gabrielson M., Chiesa F., Paulsson J., Strell C., Behmer C., Rönnow K., Czene K., Östman A., Hall P. Amount of stroma is associated with mammographic density and stromal expression of oestrogen receptor in normal breast tissues. Breast Cancer Res Treat. 2016;158:253-261. doi: 10.1007/s10549-016-3877-x.

21 Dekker P., Gunn D., McBryan T., Dirks R.W., van Heemst D., Lim F.L., Jochemsen A.G., Verlaan-de Vries M., Nagel J., Adams P.D., et al. Microarray-based identification of age-dependent differences in gene expression of human dermal fibroblasts. Mech Ageing Dev. 2012; 133: 498-507. doi: 10.1016/j.mad.2012.06.002.

22 Neville M. C. Stages in the development of mammary function. In Lactation. Physiology, Nutrition and breast feeding. Edited by Margaret C. Neville and Marianne R. Neifert. Plenun Press, New York, 1983; pages 104-116. ISBN – 13:978-1-4613-3690-7

23 Yao J., Weremowicz S., Feng B., Gentleman R.C., Marks J.R., Gelman R., Brennan C., Polyak K. Combined cDNA array comparative genomic hybridization and serial analysis of gene expression analysis of breast tumor progression. Cancer Res. 2006; 66: 4065-4078.

24 Wang X., Ghareeb W.M., Lu X., Huang Y., Huang S., Chi P. Coexpression network analysis linked H2AFJ to chemoradiation resistance in colorectal cancer. J Cell Biochem. 2019;120:10351-10362. doi: 10.1002/jcb.28319.

25 Noor A., Whibley A., Marshall C.R., Gianakopoulos P.J., Piton A., Carson AR, Orlic-Milacic M., Lionel A.C., Sato D., Pinto D., et al. Disruption at the PTCHD1 Locus on Xp22.11 in Autism spectrum disorder and intellectual disability. Sci Transl Med. 2010; 2: 49ra68. doi: 10.1126/scitranslmed.3001267.

26 Olive K.P., Jacobetz M.A., Davidson C.J., Gopinathan A., McIntyre D., Honess D., Madhu B., Goldgraben M.A., Caldwell M.E., Allard D., et al. Inhibition of Hedgehog signaling enhances delivery of chemotherapy in a mouse model of pancreatic cancer. Science. 2009;324:1457-1461. doi: 10.1126/science.1171362.

27 Kim C.H., Lim H.W., Kim J.R., Rott L., Hillsamer P., Butcher E.C.. Unique gene expression program of human germinal center T helper cells. Blood. 2004;104:1952-60.

28 Scott A.C., Dündar F., Zumbo P., Chandran S.S., Klebanoff C.A., Shakiba M., Trivedi P., Menocal L., Appleby H., Camara S., et al. TOX is a critical regulator of tumour-specific T cell differentiation. Nature. 2019 Jul;571(7764):270-274. doi: 10.1038/s41586-019-1324-y. .

29 Kato M., McDonald K.J., Khan S., Ross I.L., Vuckovic S., Chen K., Munster D., MacDonald K.P., Hart D.N. Expression of human DEC-205 (CD205) multilectin receptor on leukocytes. Int Immunol. 2006;18:857-69.

30 Jiang W., Swiggard W.J., Heufler C., Peng M., Mirza A., Steinman R.M., Nussenzweig M.C.. The receptor DEC-205 expressed by dendritic cells and thymic epithelial cells is involved in antigen processing. Nature. 1995; 375:151-155.